0026-895X/97/010155-09$3.00/0

MOLECULAR PHARMACOLOGY, **52:**155–163 (1997).

Differences in Folylpolyglutamate Synthetase and Dihydrofolate Reductase Expression in Human B-Lineage versus T-Lineage Leukemic Lymphoblasts: Mechanisms for Lineage Differences in Methotrexate Polyglutamylation and Cytotoxicity

AMY J. GALPIN, JOHN D. SCHUETZ, ERIC MASSON, YURI YANISHEVSKI, TIMOTHY W. SYNOLD, JULIO C. BARREDO, CHING-HON PUI, MARY V. RELLING, and WILLIAM E. EVANS

Departments of Pharmaceutical Sciences (A.J.G., J.D.S., E.M., Y.Y., T.W.S., M.V.R., W.E.E.) and Hematology-Oncology (C.-H.P.), St. Jude Children's Research Hospital, and the Center for Pediatric Pharmacokinetics and Therapeutics (M.V.R., W.E.E., C.-H.P., J.D.S), Colleges of Pharmacy and Medicine, University of Tennessee, Memphis, Tennessee 38101, and Division of Pediatric Hematology-Oncology, Medical University of South Carolina, Charleston, South Carolina (J.C.B.)

Received February 14, 1997; Accepted April 10, 1997

SUMMARY

Cellular accumulation of methotrexate polyglutamates (MTXPGs) is recognized as an important determinant of the cytotoxicity and selectivity of methotrexate in acute lymphoblastic leukemia (ALL). We identified a significantly lower cellular accumulation of MTXPGs in T-lineage versus B-lineage lymphoblasts in children with ALL, which is consistent with the worse prognosis of T-lineage ALL when treated with conventional antimetabolite-based therapy. Maximum MTXPG accumulation in leukemic blasts *in vivo* was 3-fold greater in lymphoblasts of children with B-lineage ALL (129 children) compared with those with T-lineage ALL (20 children) ($p < 0.01$) and was characterized by a saturable (E_{max}) model in both groups. The human leukemia cell lines NALM6 (B-lineage) and CCRF/CEM (T-lineage) were used to assess potential mechanisms for these lineage differences in MTX accumulation, revealing i) greater total and long-chain MTXPG accumulation in NALM6 over a wide range of methotrexate concentrations (0.2–100 μM), ii) saturation of MTXPG accumulation in both cell lines, with a higher maximum (E_{max}) in NALM6, iii) 3-fold higher constitutive FPGS mRNA expression and enzyme activity in NALM6 cells, iv) 2-fold lower levels of DHFR mRNA and protein in NALM6 cells, and v) 4–6 fold lower extracellular MTX concentration and 2-fold lower intracellular MTXPG concentration to produce equivalent cytotoxicity (LC_{50}) in NALM6 versus CEM. There was a significant relationship between FPGS mRNA and enzyme activity in lymphoblasts from children with newly diagnosed ALL, and blast FPGS mRNA and activity increased after methotrexate treatment. These data indicate higher FPGS and lower DHFR levels as potential mechanisms contributing to greater MTXPG accumulation and cytotoxicity in B-lineage lymphoblasts.

MTX is an antifolate that is one of the most widely used drugs for the treatment of childhood ALL. It is also used as an immunosuppressant for autoimmune and inflammatory disorders, as well as for the treatment of numerous solid tumors. Its mechanism of action is classically attributed to inhibition of DHFR-mediated regeneration of tetrahydrofolates from dihydrofolates, the latter generated as oxidation products of one-carbon transfer reactions in purine and pyrimidine synthesis. MTX is a substrate for FPGS, which catalyzes the sequential addition to MTX of one to several glutamate moieties, forming polyglutamate derivatives (MTXPGs), which are better retained intracellularly (1, 2). Due to their longer cellular retention (3), MTXPGs can accumulate to intracellular levels that substantially exceed cellular DHFR binding capacity, leading to complete inhibition of tetrahydrofolates biosynthesis from dihydrofolates (4). Furthermore, unlike the parent drug, longer chain forms of MTXPGs (e.g., four to six glutamate residues) inhibit enzymes involved in *de novo* purine synthesis (i.e., aminoimi-

This study was supported in part by National Institutes of Health/National Cancer Institute Grant R37-CA36401, Leukemia Program Project Grant CA20180, and Cancer Center CORE Grant CA21765; a State of Tennessee Center of Excellence grant; and the American Lebanese Syrian Associated Charities.

ABBREVIATIONS: MTX, methotrexate; ALL, acute lymphoblastic leukemia; CEM, human T-lineage leukemia cell line (CEM/CCRF); DHFR, dihydrofolate reductase; FBS, fetal bovine serum; FPGS, folylpolyglutamate synthetase; GAT, glycine, adenosine, thymidine; HDMTX, high-dose methotrexate; LC_{50}, concentration producing 50% cell kill; LC_{90}, concentration producing 90% cell kill; LDMTX, low-dose methotrexate; MTXPG, methotrexate polyglutamate; $MTXPG_x$, methotrexate, where x is number of glutamyl residues; NALM6, human B-lineage leukemia cell line; PCR, polymerase chain reaction.

dazole carboxamide ribonucleotide transformylase, glycinamide ribonucleotide transformylase) and thymidylate synthase (1, 5). Thus, intracellular formation of MTXPGs may enhance the effects of MTX by multiple mechanisms.

Failure to accumulate MTXPGs has been associated with MTX resistance in breast cancer, squamous cell carcinoma, leukemia, and other malignant cell lines (6–8), with decreased FPGS-catalyzed polyglutamylation representing one of several mechanisms influencing MTX accumulation, cytotoxicity, and selectivity (9–11). Other potential mechanisms of MTX resistance include decreased MTX cell entry due to impaired membrane transport (12), altered levels or structure of target enzymes (e.g., DHFR) (9, 13, 14), and enhanced hydrolytic cleavage of MTXPGs (15).

Greater intracellular accumulation of MTXPGs has been documented for leukemic lymphoblasts isolated from children versus adults (16), hyperdiploid versus nonhyperdiploid ALL (17, 18), and B-lineage versus T-lineage ALL (16, 18); in each comparison, the former group with higher intracellular MTXPGs generally has a better prognosis. Whitehead *et al.* (17) observed that lower *ex vivo* lymphoblast accumulation of MTXPGs was predictive of unfavorable clinical outcome for children with B-lineage ALL. Our studies established these differences *in vivo*, documenting 3-fold greater accumulation of total and long-chain MTXPGs in B-lineage versus T-lineage lymphoblasts isolated from patients after treatment with MTX (18). We further demonstrated an increase in lymphoblast FPGS activity during MTX treatment, with a significantly greater increase in B-lineage versus T-lineage lymphoblasts (19). We have more recently shown that greater lymphoblast MTXPG accumulation is associated with greater antileukemic effects in children with newly diagnosed B-lineage ALL (20). The current study was conducted to elucidate mechanisms underlying these lineage differences in lymphoblast MTXPG accumulation and cytotoxicity and to provide new insights for the design of optimal MTX treatment strategies for these subtypes of childhood ALL.

Experimental Procedures

Materials. Adenosine, glycine, methotrexate, thymidine, salmon sperm DNA, sodium chloride, sodium triacetate, and sodium lauryl sulfate were purchased from Sigma Chemical (St. Louis, MO). [^{3}H]Methotrexate was obtained from Moravek (Brea, CA), and scintillation cocktail was from IN/US systems (Tampa, FL). Phenol, formamide, and formaldehyde were supplied by Fisher Scientific (Springfield, NJ). Guanidium-isothiocyanate, phosphate buffered saline, L-glutamine, and Moloney murine leukemia virus reverse transcriptase (Superscript) were from Life Technologies (Grand Island, NY). 5′-DNA-terminal labeling kits were purchased from Life Technologies (Bethesda, MD). RPMI-1640 was obtained from Biowhittaker (Walkersville, MD). Nytran membrane was obtained from Micron Separations (Cleveland, OH). Random priming radiolabeling kits and probe purification columns were purchased from Stratagene (Palo Alto, CA). DNA restriction enzymes, plasmid DNA extraction kits, dNTPs, RNasin, T4 DNA ligase, and Klenow fragment of *DNaseI* were purchased from Promega (Madison, WI). Radioisotopes [α-^{32}P]dCTP and [γ-^{32}P]ATP were obtained from Dupont-NEN (Bakersfield, CA). DNA *Taq* polymerase (Amplitaq) and PCR 10× buffer were purchased from Perkin-Elmer Cetus (Norwalk, CT).

Oligonucleotide and cDNA probes. A cDNA containing the full-length coding sequence for murine dihydrofolate reductase, pDHFR7, was kindly provided by Dr. Stanley N. Cohen (Stanford University) and used as previously described (21). An oligonucleotide, designated h28AS, was synthesized as antisense to human 28S ribosomal RNA extending from bases 4571–4600,[1] with the sequence 5′-TCTGACTTAGAGGCGTTCAG TCATAATCC-3′.

A cDNA probe for human FPGS, encompassing bases 1489–1708 of the FPGS cDNA sequence (22)[2] corresponding to exon 15, was derived through PCR, as follows. Synthetic oligonucleotide primers (Operon Technologies; San Francisco, CA) of sequence 5′-GTCTTCAGCTGCATTTCACATGCCTTGCAATGGA-3′ and 5′-CTACTGGGAC AGTGCGGGCTCCAGCAGCTT-3′ are hereafter referred to as S1489 and AS1708, respectively. First-strand cDNA was synthesized by reverse transcription of 2 μg of patient-derived lymphoblast total RNA in 20-μl reactions containing 200 units of Moloney murine leukemia virus reverse transcriptase, 200 ng of random hexamers, 20 units of RNasin, and 1 mM concentration of each dNTP in a buffer of 50 mM KCl, 10 mM Tris·HCL, pH 8.3, 1.5 mM $MgCl_2$, and 0.001% (w/v) gelatin as previously described (27). PCR amplification was performed in 100-μl reaction mixtures containing 50–600 ng of first-strand template, 200 μM concentrations of dNTPs, 100 pmol each of S1489 and AS1708 primers, and 2.5 units of DNA *Taq* polymerase, in buffer as above. Mixtures were overlaid with mineral oil, were denatured initially for 3.5 min at 95°, underwent 40 amplification cycles (denaturation at 94° for 2 min, annealing at 52° for 1 min, extension at 72° for 2 min), were renatured at 72° for 10 min, and then were cooled at 25° for 2 min. The 220-bp amplification product was isolated using GeneClean, rendered blunt by the use of Klenow fragment, and ligated into the *Sma*I site of M13mp19 (Pharmacia) and single-stranded phage prepared as a template for DNA sequence analysis. Automated fluorescence sequencing established that this FPGS cDNA was identical to the published FPGS cDNA.[2] The FPGS cDNA was subcloned into pGEM-7Zf+ (Promega), and the insert was isolated by digestion of the plasmid with *Eco*RI and *Hin*dIII.

FPGS activity. Cytosol was prepared from $\geq 5 \times 10^6$ cells that had been harvested, cryopreserved, and processed as previously described (19). FPGS activity determinations were performed according to the [^{3}H]glutamic acid incorporation microassay, previously reported in detail (24). Reaction product values (dpm) were converted to pmol product equivalents, normalized to sample protein content as determined by the Bradford dye-binding procedure, and expressed as pmol/mg of protein/hr.

MTX and MTXPG quantification. MTX concentrations were measured in patient serum and *in vitro* incubation medium with the Abbottbase TDx-FPIA II assay (Abbott Diagnostics, Irving, TX). Intracellular concentrations of MTX and its polyglutamylated derivatives (MTXPGs) were determined in leukemia cells harvested after *in vitro* exposure to MTX and in patient peripheral blood or bone marrow lymphoblasts after *in vivo* exposures to MTX, as previously described (18, 20). Harvested cell pellets ($\sim 5 \times 10^6$ cells) were freshly extracted for MTXPGs; individual polyglutamate fractions were separated by high performance liquid chromatography and then quantified by a competitive DHFR-binding REA method (25). Results (pmol) were normalized to 10^9 cells, with the lower limit of detection being 20 pmol/10^9 cells.

A radioisotopic method of MTXPG detection was also used for *in vitro* experiments with NALM6 and CEM cells, in which [^{3}H]MTXPG accumulation was assessed. After incubation with 1.0 μM [^{3}H]MTX (specific activity, 10 mCi/μmol), cell harvests were washed, pelleted, and extracted for MTXPGs, which were then separated by high performance liquid chromatography, as previously described (18). Radioactivity (dpm) was determined for each polyglutamate by in-line scintillation counting, converted to [^{3}H]MTXPG pmol equivalents (based on specific activity of 10 mCi/μmol), and normalized to 10^9 cells, as described above.

Cell lines and culture conditions. The human T-lineage ALL line CEM/CCRF (CEM) was obtained from American Type Culture

[1] GenBank accession no. M11176.
[2] GenBank accession no. M98045.

Collection (Bethesda, MD); it is $CD3^+CD10^-$, diploid, and without translocations. The human early pre-B ALL cell line NALM6 was kindly provided by Dr. Fatih Uckun (University of Minnesota); it is diploid, $CD10^+CD19^+$, cytoplasmic μ-positive, and without translocations (26). Cells were routinely cultured in RPMI-1640 with 10% heat-inactivated FBS and 2 mM L-glutamine at 37° in O_2 95%/CO_2 5% and 95% humidity. Flasks were subcultured at one fourth to one fifth density every 3–4 days. When medium was supplemented with GAT, the final medium concentrations were 670 μM glycine, 37 μM adenosine, and 41 μM thymidine.

Percent S-phase. Percentage of cells in S-phase was determined by DNA histogram analysis of propidium iodide-stained nuclei on fresh or cryopreserved aliquots of 10–20 $\times$ 10^6 cells, as previously described (18).

MTX *in vitro* incubations. MTX *in vitro* exposures were begun at the mid-late log growth phase (i.e., 40–56 hr after splitting, at cell densities of 1.0–2.0 $\times$ 10^6/ml). The routine culture medium (above) with GAT supplement was used for studies of MTXPG accumulation. Medium without GAT supplement was used for determinations of FPGS activity and for RNA isolation to assess changes in FPGS and DHFR mRNA. Cells were suspended in fresh medium at a density of 1–1.5 $\times$ 10^6/ml in flasks or six-well plates at final MTX concentrations ranging from 0.002 to 100 μM (NALM6) or 0.01 to 100 μM (CEM). For consistency with *in vivo* studies in patients (18–20), [^{3}H]MTX incubations were conducted in minimum essential medium supplemented with 2 mM L-glutamine, 10% heat-inactivated FBS, and GAT at cell densities of 5 $\times$ 10^6/ml.

MTX cytotoxicity studies. Cytotoxicity was assessed in RPMI-1640 with 2 mM L-glutamine and dialyzed FBS 10% (heat-inactivated). Viabilities were assessed after 24-hr incubation with MTX and after subsequent culture in MTX-free medium for an additional 24 hr (i.e., 48-hr time point). Cell aliquots (750 μl) were harvested after different MTX incubations and prepared for flow cytometric analysis (Becton-Dickinson), using standard methods. Cell viability was determined by flow cytometric analysis of forward and side light scatter; then, viable cell counts per standard flow rate and time were expressed as a percent cell viability relative to untreated cells (27). Control cell viability, without MTX, was consistently >90%. Percent cell viability was plotted against log MTX concentration (0.1 nM to 100 μM) and those MTX concentrations producing 50% cell kill (LC_{50}) and 90% cell kill (LC_{90}) were determined from survival curve fitting to the data using ALLFIT curve-fitting software (28).

RNA extraction and Northern blot analysis of FPGS and DHFR. Total RNA was extracted from freshly isolated patient lymphoblasts and cell line samples, according to the method of Chomcynski (29). The RNA yields ranged from 10 to 25 μg of RNA/10^7 patient lymphoblasts and from 20 to 40 μg of RNA/10^7 cultured cells. Total RNA was size-fractionated by gel electrophoresis and transferred electrophoretically to a positively charged membrane (Magna NT; Micron Separations, Westboro, MA). Transcript sizes were estimated by log-linear interpolation from the 28S (4.9 kb) and 18S (1.95 kb) migration distances.

cDNA probes were radiolabeled by random priming with [^{32}P]dCTP, and oligonucleotides were end-labeled with T_4 polynucleotide kinase. Unincorporated nucleotides were removed by Nuctrap (Stratagene), and probe specific activity was determined. Northern blot membranes were successively hybridized with the FPGS cDNA, DHFR-7 cDNA, and h28S; each probe was removed by immersion in boiling water (1–2 min) before reprobing. Prehybridization and hybridization protocols were followed as previously described (30) using solutions of formamide 50% (cDNAs at 42°) or 15% content (oligonucleotides at 37°). Membrane washes proceeded from 2$\times$ standard sodium citrate/0.2% sodium dodecyl sulfate at 42° to final stringencies of 2$\times$ standard sodium citrate/0.2% sodium dodecyl sulfate at 65° (FPGS cDNA), 60° (DHFR cDNA), and 70° (h28Sr). The hybridization signals were scanned by PhosphorImager (model 425F; Molecular Dynamics, Sunnyvale, CA) and quantified by ImageQuant software version 3.3 (Molecular Dynamics). FPGS and DHFR signal values were normalized to the corresponding h28S signal intensity to adjust for RNA loading and integrity.

Western blot analysis of DHFR. Cytosol was prepared from logarithmically growing CEM and NALM6 cells, and the relative amount of DHFR was determined by varying the amount of protein blotted, as previously described (31). The amount of actin protein was used to assess variations in protein and loading in CEM and NALM6. Densitometric quantification was used to assess difference in DHFR signals. To account for nonlinearity of the assay, a sigmoid E_{max} model,

$$E = \frac{E_{max} \times C^N}{EC_{50}^N + C^N}$$

was simultaneously fit to the DHFR signal obtained from Western blot versus total cell protein loaded for each lane. E_{max} and N, as properties of the assay, were the same for both experimental curves. The ratio between intracellular DHFR concentrations normalized to total cellular protein was determined as the ratio of EC_{50} coefficients of the fitted sigmoidal curves. ALLFIT software (28) was used to fit sigmoidal curves to these data.

Human subjects. After informed written consent by parents or legal guardians, patients with newly diagnosed ALL were randomized to a treatment protocol previously described in detail (18). The methods for diagnosis of ALL, determination of immunophenotype, and administration of MTX have also been previously described (18).

Relation between MTX plasma concentration and MTXPG accumulation in lymphoblasts of patients treated with MTX. The concentrations of MTX in plasma and of MTXPGs in leukemic lymphoblasts of children with newly diagnosed ALL were determined as previously described (18). The relation between MTX plasma concentration and MTXPG accumulation in lymphoblasts was assessed using the steady state MTX plasma concentration measured either at the end of a 24-hr intravenous infusion of HDMTX (1000 mg/m^2) or the peak steady state concentration after oral LDMTX (30 mg/m^2 q6h $\times$ 6). These data were analyzed by fitting an E_{max} model to the intracellular versus extracellular concentration data and estimating the maximum level of intracellular accumulation (E_{max}) separately for patients with T-lineage and B-lineage ALL.

Modeling and statistics. Intracellular MTXPG accumulation after 24-hr exposure at extracellular MTX concentrations ranging from 0.1 to 100 μM was modeled using the Michaelis-Menten equation, and extracellular MTX concentrations required to achieve 95% of maximum intracellular MTXPG level were obtained from model parameters for each cell line. The Mann-Whitney U test was used for between-group comparisons.

Results

Relation between MTX plasma concentration and MTXPG accumulation in lymphoblasts of patients treated with MTX. MTXPG accumulation was determined in a total of 149 children with newly diagnosed ALL: 129 with B-lineage ALL and 20 with T-lineage ALL. In the initial 101 children on this study, we observed greater MTXPG accumulation in hyperdiploid (>50 chromosomes) than nonhyperdiploid lymphoblasts among children with B-lineage ALL (18). Because hyperdiploidy is rare in T-lineage ALL, the comparison of lineage differences in MTXPG accumulation was restricted to the 114 patients with nonhyperdiploid ALL (96 B-lineage, 18 T-lineage). In these patients, long-chain $MTXPG_{4-6}$ accumulation was significantly greater in lymphoblasts of patients with B-lineage ALL than in those with T-lineage ALL after treatment with either HDMTX (median, 968 pmol/10^9 blasts versus 315 pmol/10^9 blasts, $p = 0.018$) or LDMTX (median, 260 pmol/10^9 blasts versus 75 pmol/10^9

blasts, $p = 0.0053$). It should be noted that lymphoblast concentrations in patients were measured 44 hr from the start of MTX therapy (i.e., 20 hr after the end of a 24-hr MTX IV infusion or 14 hr after the last oral dose of MTX). Due to interpatient variability in MTX systemic clearance, there was a wide range of MTX steady state plasma concentrations in these patients, permitting assessment of the relation between MTXPG accumulation in lymphoblasts and extracellular MTX concentrations. As depicted in Fig. 1, the data were characterized by an E_{max} model, with an estimated maximum *in vivo* accumulation of long-chain MTXPGs that was 3-fold greater in lymphoblasts from patients with B-lineage ALL (1568 ± 265 pmol/10^9 blasts) compared with patients with T-lineage ALL (431 ± 117 pmol/10^9 blasts) ($p < 0.01$).

Lineage differences in accumulation and loss of total and long-chain MTXPGs in human leukemic cell lines. Fig. 2 depicts the accumulation and retention profiles of MTXPGs during and after a 24-hr exposure to 1 μM [^{3}H]MTX in B-lineage and T-lineage lymphoblasts. During the early accumulation phase (4 hr), $MTXPG_{4-6}$ predominated in NALM6 (B-lineage), whereas shorter-chain MTXPGs predominated in CEM cells (T-lineage). Cellular accumulation of total and long-chain MTXPGs was greater in NALM6 than in CEM at all time points (Fig. 2). After removal of extracellular MTX, the pentaglutamate became the major form of intracellular MTX at 24 hr in both cell lines (data not shown). Intracellular MTXPGs (long-chain and pentaglutamate) decreased more rapidly in NALM6 ($t_{½}$ = 15 hr for $MTXPG_{4-6}$ and 14 hr for $MTXPG_5$) than in CEM ($t_{½} \sim$ 56 hr for $MTXPG_{4-6}$ and ~ 88 hr for $MTXPG_5$) after removal of extracellular MTX; however, the total intracellular level of MTXPGs remained higher in NALM6 at all time points tested.

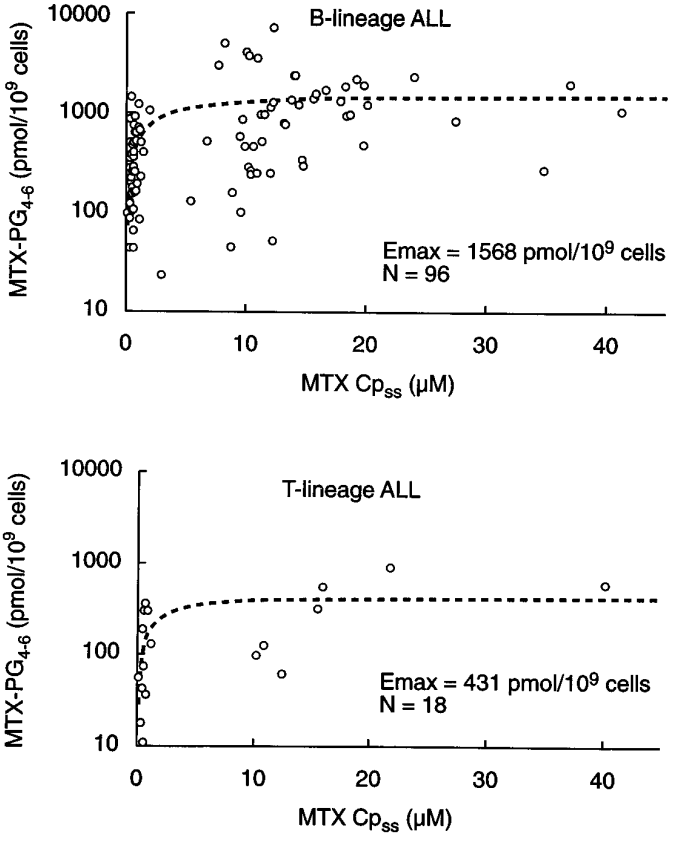

Fig. 1. Relation between lymphoblast concentration of long-chain MTXPGs (glu4–6) measured 44 hr after starting either LDMTX (30 mg/m^2 oral q6h ×6) or HDMTX (1000 mg/m^2 intravenous over 24 hr) and the steady state MTX plasma concentration in each patient. *Top*, nonhyperdiploid B-lineage ALL (96 patients). *Bottom*, nonhyperdiploid T-lineage ALL (18 patients). *Dashed lines*, best fit of an E_{max} model to the data, estimating maximum accumulation of 1568 pmol/10^9 blasts in B-lineage ALL versus 431 pmol/10^9 blasts in patients with T-lineage ALL.

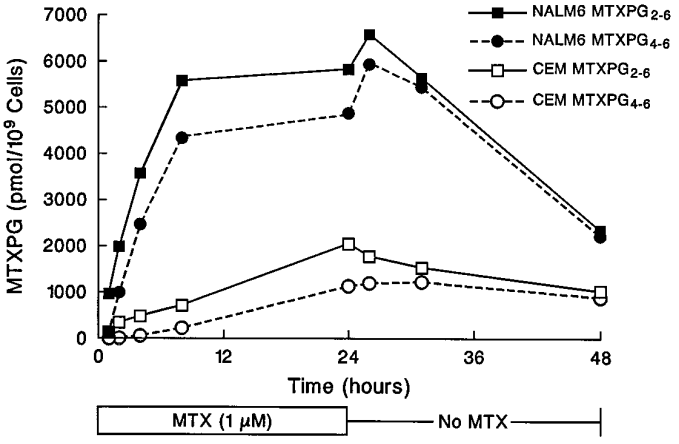

Fig. 2. Time course of MTXPG accumulation and retention in NALM6 (B-lineage) and CEM (T-lineage) cell lines during 24-hr continuous exposure to 1 μM [^{3}H]MTX and for 24 hr after extracellular MTX removal.

Lineage differences in time and concentration effects on MTXPG accumulation *in vitro*. Fig. 3 depicts differences in long-chain MTXPGs (i.e., glu4–glu6) accumulation between NALM6 and CEM after 4, 8, or 24 hr of incubation at concentrations of MTX ranging from 0.2 to 5.0 μM. Lineage differences were evident for both long-chain and total MTXPGs at all concentrations and times tested. Prolongation of exposure and increased extracellular MTX increased MTXPG accumulation in both cell lines; however, the impact differed for NALM6 versus CEM cells. Extending the duration of MTX exposure beyond 8 hr increased MTXPG accumulation appreciably in CEM at all concentrations tested, but this was evident for NALM6 only at the lowest MTX concentration tested (0.2 μM), with little or no further increase when exposure was extended beyond 8 hr for either 1.0 or 5.0 μM.

Lineage differences in maximum accumulation of total and long-chain MTXPGs in vitro. After 24-hr exposure at extracellular MTX concentrations ranging from 0.1 to 100 μM, total intracellular MTXPG concentrations reached 95% of maximum (IC_{95}) at 59 μM (standard error = 17) for NALM6 and 66 μM (standard error = 28) for CEM (Fig. 4). For long-chain $MTX\text{-}PG_{4-6}$, the extracellular concentration producing the IC_{95} was 34 μM (standard error = 11) for NALM6 versus 48 μM (standard error = 16) for CEM (Fig. 4). Although the extracellular MTX concentrations that produced 95% of maximum MTXPG accumulation differed by ≤1.5-fold in these two cell lines, maximum intracellular $MTXPG_{4-6}$ concentrations were 6 times higher in NALM6 than in CEM (21,000 versus 3,480 pmol/10^9 cells; $p < 0.001$).

FPGS mRNA expression and activity in B-lineage (NALM6) and T-lineage (CEM) ALL cell lines. FPGS mRNA transcript size (2.2 kbp) did not differ between T-lineage (CEM) and B-lineage (NALM6) cells (Fig. 5A). The

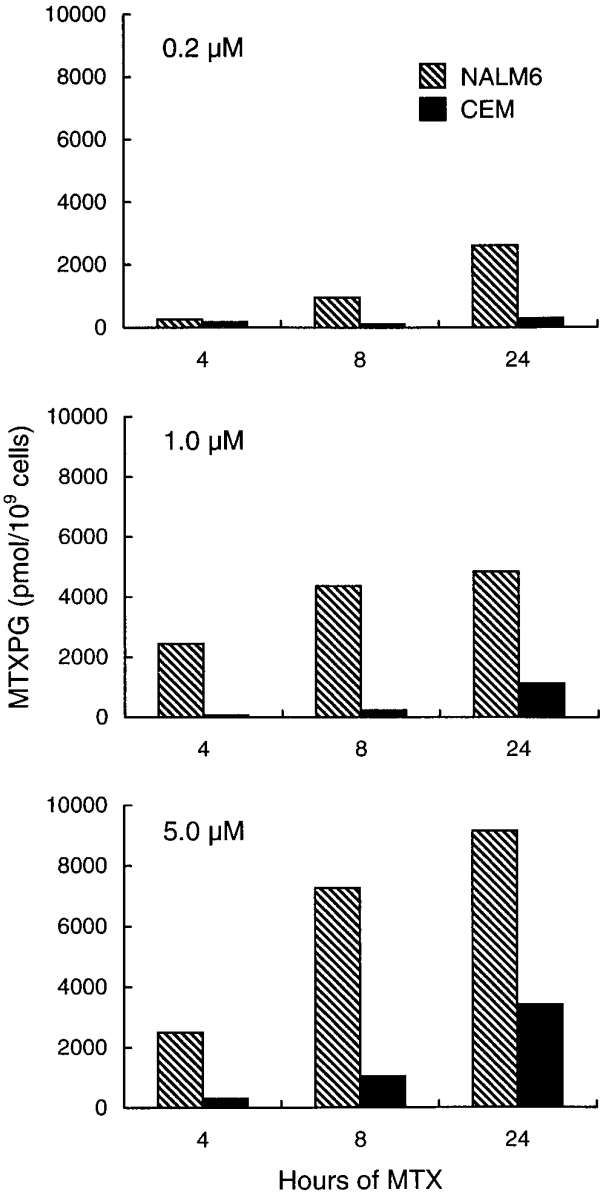

Fig. 3. Concentration and time dependence of intracellular long-chain MTXPGs (glu4–glu6) accumulation in human B-lineage (NALM6) and T-lineage (CEM) leukemia cell lines. MTXPG intracellular fractions were determined as described in Methods, after continuous exposure to MTX at the concentrations and times indicated.

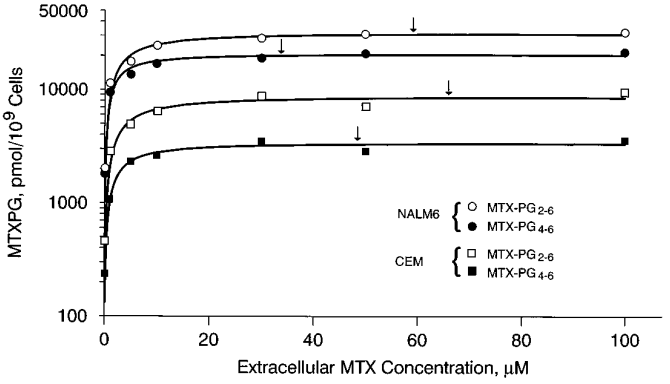

Fig. 4. Intracellular accumulation of total (○ and □) and long-chain (● and ■) MTXPGs in B-lineage NALM6 (● and ○) and T-lineage CEM (□ and ■) human leukemia cell lines after 24-hr incubation with extracellular MTX at concentrations of 0.1–100 μM. *Arrows*, extracellular concentration at which intracellular accumulation attains 95% of maximum.

mean constitutive level of FPGS mRNA in untreated NALM6 was ~3-fold greater than in CEM (Fig. 5A, $p < 0.01$). Similarly, the constitutive FPGS activity was 3–4-fold higher in NALM6 [mean 1480 pmol/hr (standard deviation = 312) versus 370 pmol/hr (standard deviation = 81; $p < 0.01$) (Fig. 5B)]. Consistent with the higher FPGS activity in NALM6, the accumulation of long-chain $MTXPG_{4-6}$ was >4-fold higher in NALM6 versus CEM cells (Fig. 3) after identical exposures to MTX (e.g., 5 μM for 24 hr). The percentage of untreated cells in S-phase was similar in NALM6 and CEM (~45% in both); thus, the 3-fold greater FPGS mRNA in NALM6 cannot be explained by a difference in the percentage of cells in S-phase.

Base-line levels of DHFR mRNA and protein in NALM6 and CEM. Before MTX incubations were started (i.e., mid-log phase), DHFR mRNA base-line levels averaged ~1.7-fold higher in CEM than NALM6 ($p < 0.01$). As depicted in Fig. 6, DHFR protein levels were ~2.2-fold higher in CEM than NALM6 when normalized to total cellular protein loaded and 2.8-fold higher in CEM when normalized to actin protein.

Lineage differences in FPGS and DHFR mRNA after MTX exposure. During MTX exposure (24-hr exposure to 0.05–5 μM MTX), FPGS mRNA transiently increased in both NALM6 and CEM. Fig. 7 illustrates differences in the magnitude of observed FPGS mRNA increases during exposure to three MTX concentrations (0.2, 1.0, 5.0 μM). For both NALM6 and CEM, MTX produced a dose-dependent increase in FPGS mRNA, and the increase in FPGS mRNA was significantly greater in NALM6 versus CEM at lower MTX concentrations ($p = 0.03$ at 0.2 μM). Furthermore, the maximal "induction" of FPGS mRNA occurred earlier in NALM6 (2–8 hr) than in CEM (8–15 hr). Even after maximal increases, the level of FPGS mRNA was consistently lower in CEM compared with NALM6.

When these same blots were stripped and reprobed with a DHFR cDNA, an increase in DHFR mRNA was observed in both cell lines at each MTX concentration tested. However, base-line levels were significantly higher ($p < 0.01$), and the fold increases in DHFR mRNA during MTX exposures tended to be higher ($p = 0.08–0.12$) in CEM than in NALM6 (Fig. 7). In both lineages, as MTX concentration increased, the "induction" of DHFR mRNA diminished, a pattern that was in contrast to FPGS.

Relationships in vivo among lymphoblast FPGS mRNA, enzyme activity, and MTX exposure in patients. Fig. 8 depicts the relationship between FPGS mRNA levels and FPGS activity in ALL blasts isolated from newly diagnosed patients (11 samples in six patients) during single-agent MTX treatment. Maximal *in vivo* changes in FPGS mRNA observed in lymphoblasts isolated from these patients after 6–44 hr of MTX treatment was greater in leukemia cells isolated from patients with B-lineage ALL receiving HD-MTX, which is consistent with the *in vivo* lineage differences in FPGS activity we observed in ALL blasts (19).

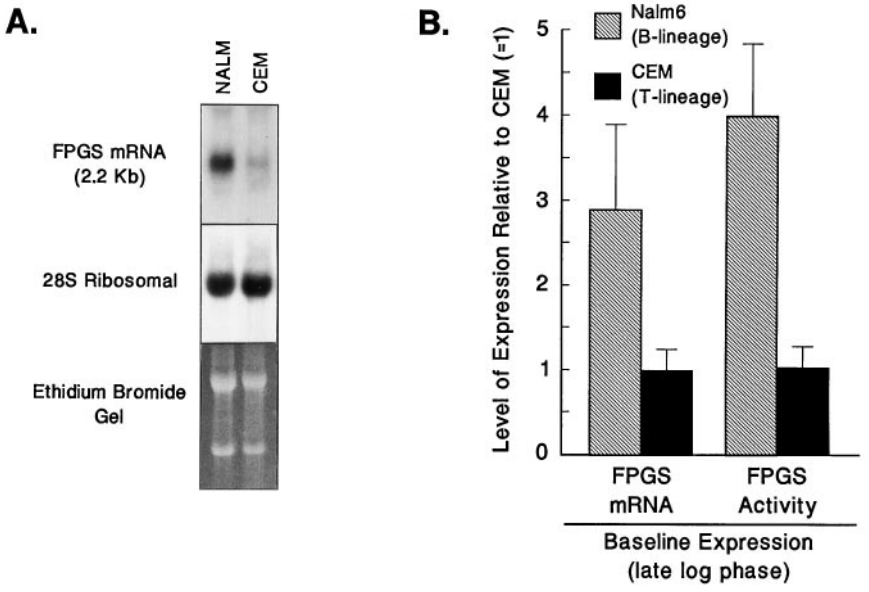

Fig. 5. A, Northern blot analysis of FPGS mRNA in human B-lineage (NALM6) and T-lineage (CEM) leukemia cells. Total RNA (20 μg) extracted from logarithmically growing cells was analyzed by Northern blot analysis with FPGS cDNA and 28S rRNA probes, as described in Methods. B, Lineage differences in FPGS mRNA and activity in NALM6 and CEM leukemia cell lines. RNA levels were measured by Phosphorimaging, normalizing FPGS signal to 28S signal, and expressing these relative to the level in CEM cells (given a value of 1). Enzyme activities were determined on samples collected concurrently with RNA, from logarithmically growing cells. Values represent the median ± standard deviation of six or seven replicates.

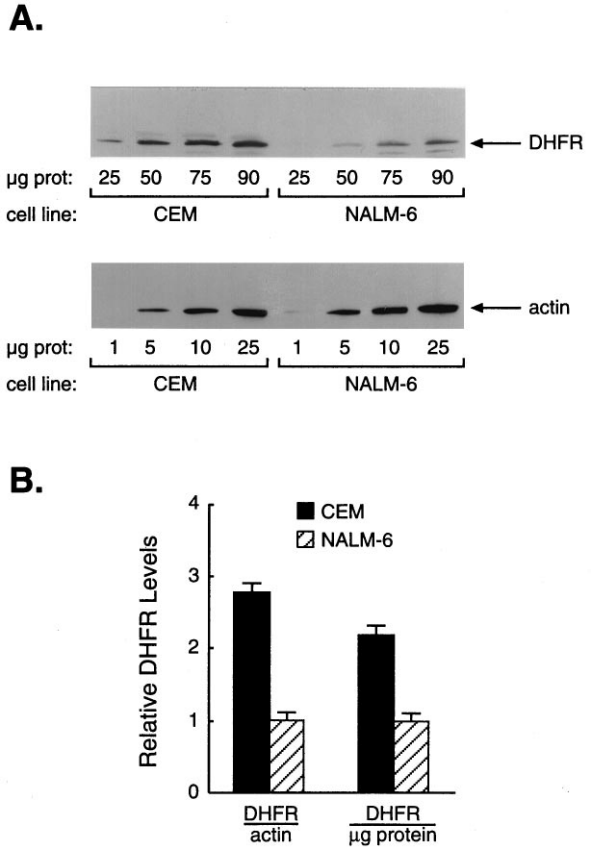

Fig. 6. A, Western blot of DHFR and actin isolated from logarithmically growing CEM (T-lineage) or NALM6 (B-lineage) human leukemia cells. The amount of total cellular protein loaded is indicated for each lane. B, Densitometric estimate of the amount of DHFR protein normalized to either actin (■) or total protein (▨) loaded, depicting the amount of DHFR in CEM relative to NALM6 (arbitrarily set to a value of 1).

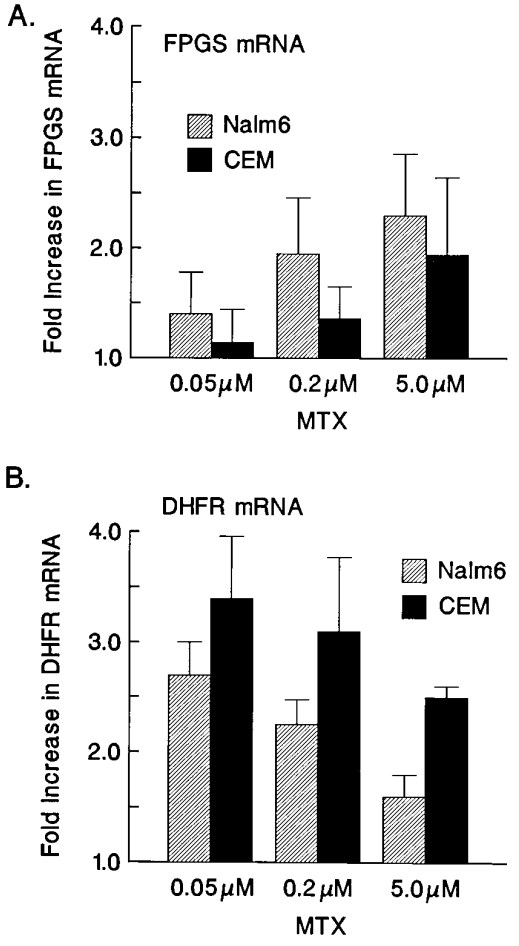

Fig. 7. Fold-increase from pretreatment levels of FPGS mRNA (A) and DHFR (B) in NALM6 (▨) versus CEM (■) leukemia cells during 24-hr incubation with MTX (0.05, 0.2, and 5.0 μM). *Bars*, maximum observed increases based on the mean of four replicate experiments (mean ± standard deviation indicated).

Relationship of extracellular MTX concentration and intracellular MTXPG accumulation to cytotoxic effects. After 24-hr exposure to MTX, the extracellular MTX LC_{50} was ~5-fold higher for CEM (32–37 nM) than for NALM6 (6–8 nM) (Fig. 9). Only after 48 hr was LC_{90} achieved consistently in both lines, requiring 15-fold higher extracellular MTX concentrations in CEM (153 nM) than in NALM6 (10.2 nM). Analysis of the intracellular MTXPGs at the LC_{50}

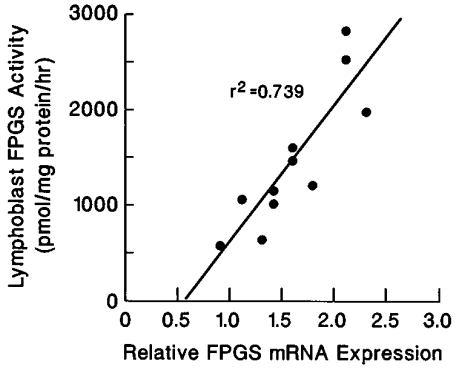

Fig. 8. Relationship between lymphoblast FPGS mRNA levels and corresponding enzyme activity in lymphoblasts from six children with newly diagnosed ALL who were receiving single-agent MTX therapy. Total RNA (18 μg) extracted from lymphoblasts was analyzed by Northern blot, and the 28S-normalized FPGS hybridization signals were expressed relative to a control NALM6 RNA. FPGS activity was also determined on a fraction of each lymphoblast collection, as described in Experimental Procedures. Samples were collected before and over the 44-hr period from the start of MTX therapy (~0, 6, 10, 23, or 44 hr). All samples were obtained before leucovorin rescue.

and LC_{90} revealed that CEM required ~2-fold higher intracellular $MTXPG_{4-6}$ levels than NALM6 to achieve comparable cytotoxicity (Fig. 10).

Discussion

A higher percentage of children with B-lineage ALL are cured with antimetabolite-based chemotherapy compared with children with T-lineage ALL (32). More recent studies indicate that comparable cure rates can be attained with more aggressive treatment regimens, but these treatments are associated with greater toxicity (33). Thus, a more complete understanding of the biochemical and molecular bases for lineage differences in treatment sensitivity may provide insights for designing more effective but less toxic therapy for these two subtypes of ALL. To that end, we used the human leukemia cell lines NALM6 (B-lineage) and CEM (T-lineage) as model systems to investigate mechanisms for differences in MTX polyglutamylation and cytotoxicity in B-lineage and T-lineage lymphoblasts.

The current study established that constitutive FPGS mRNA and activity are greater in the human B-lineage NALM6 cell line compared with the human T-lineage CEM cell line, which is consistent with lineage difference in FPGS activity in ALL blasts isolated from patients. Furthermore, FPGS mRNA increased after MTX treatment in both cell lines but to a significantly greater extent in the B-lineage NALM6 cells. These findings indicate increased FPGS mRNA as a basis for greater FPGS activity and MTXPG accumulation in the B-lineage NALM6 cells, providing a mechanism for our previous *in vivo* finding of greater increases in FPGS activity in B-lineage blasts after MTX treatment (19). Differences in FPGS activity are known to exist among normal tissues, with FPGS activity highest in liver and low or undetectable in brain, muscle, kidney, and circulating erythrocytes, granulocytes, and lymphocytes (34, 35). FPGS activity has also been linked to cell proliferation, as a 4-fold increase in FPGS mRNA occurs after phytohemagglutinin stimulation of human lymphocytes (36). There also is evidence of developmental regulation of FPGS; activity in rat liver and brain is higher during embryogenesis compared with the postnatal period (35). Furthermore, we previously documented higher FPGS activity in leukemic lymphoblasts (ALL) compared with leukemic myeloblasts (AML) and in normal lymphoid progenitors versus myeloid progenitors (19). The molecular mechanisms regulating FPGS expression in normal tissues and leukemic lymphoblasts have not been elucidated to date, representing an important area for future investigation.

In the current study, a difference was also observed in the rate of decrease of total and long-chain MTXPGs in NALM6 versus CEM cells after removal of MTX from the extracellular medium (Fig. 2). Interestingly, the rate of decrease was faster for NALM6 compared with CEM, indicating that slower hydrolysis of MTXPGs (by folylpolyglutamate hydrolase) was not the basis for greater accumulation of long-chain MTXPGs in NALM6 cells.

A modest but statistically significant difference was also found for DHFR mRNA and protein levels, with B-lineage lymphoblasts (NALM6) having a 2-fold lower level of DHFR protein. Because DHFR is a primary target for MTX and maintaining intracellular MTX concentrations above DHFR is considered essential for cytotoxicity (37), the 2-fold higher DHFR levels in CEM may explain the need for 2-fold higher intracellular MTXPG concentrations to produce equivalent cytotoxicity (i.e., LC_{50} or LC_{90}). Thus, the decreased MTX sensitivity of CEM cells, as shown by the 5-fold higher extracellular MTX concentration to produce equivalent cytotoxicity (LC_{50}), could be explained by the combination of 2–3-fold lower MTXPG accumulation and 2-fold higher DHFR levels in CEM versus NALM6. Likewise, at 200 nM, an extracellular MTX concentration near the CEM LC_{90} (153 nM), intracellular accumulation of $MTXPG_{4-6}$ was ~7-fold lower in CEM than in NALM6 (Fig. 2). When the 7-fold lower intracellular accumulation of MTXPGs is coupled with the 2-fold higher intracellular MTXPG requirement for 90% cell kill, the 15-fold greater extracellular LC_{90} in CEM versus NALM6 is not surprising.

The results of the current study have thus elucidated two biochemical differences between a human B-lineage and a human T-lineage leukemia cell line: higher FPGS expression and lower DHFR levels in the NALM6 B-lineage lymphoblasts compared with CEM cells. Because low FPGS activity (6- 8) or high DHFR levels (9) have been documented in cells selected for MTX resistance, these differences provide mechanistic insights to explain the higher intracellular accumulation of MTXPGs in B-lineage lymphoblasts and their greater sensitivity to MTX cytotoxicity compared with T-lineage lymphoblasts.

One therapeutic implication is that patients with T-lineage ALL may require a higher dosage of MTX to achieve optimal intracellular accumulation of MTXPGs. The current data indicate that 24-hr exposure to ~48 μM MTX achieved 95% maximum accumulation of long-chain MTXPGs in T-lineage CEM lymphoblasts compared with ≈34 μM for B-lineage NALM6 lymphoblasts. Although one must use caution when extrapolating from *in vitro* to *in vivo* concentrations, a MTX dosage of ~3.5 g/m^2 (500 mg/m^2 loading dose followed by 3.0 g/m^2 over 24 hr) would be required to achieve 48 μM MTX versus 2.5 g/m^2 (500 mg/m^2 plus 2.0 g/m^2 over 24 hr) to achieve 34 μM steady state plasma concentrations in a child with ALL, assuming a typical MTX plasma clearance of 100

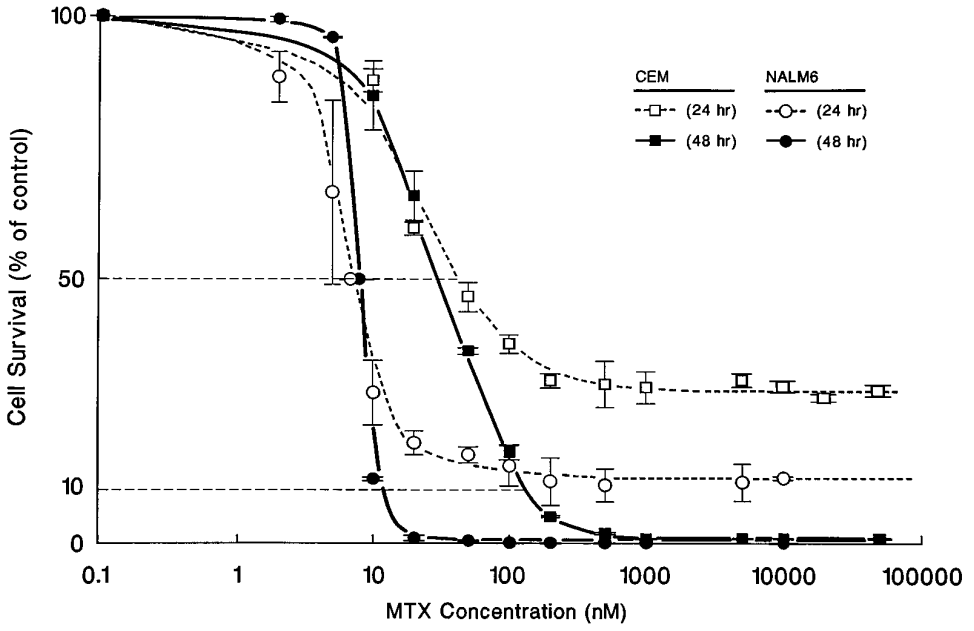

Fig. 9. MTX cytotoxicity curves demonstrating lower LC_{50} and LC_{90} values for NALM6 than CEM after 24-hr exposure to MTX. Cells were continuously incubated for 24 hr in the presence of MTX (2–50,000 nM) under "salvage-free" conditions (i.e., without GAT; see Methods). Cell viability was determined by flow cytometric analysis at the end of the 24-hr incubation and at 24 hr after return to MTX free medium (i.e., 48 hr). A sigmoid model was fit to the data (median viability of two to four replicates at each concentration) using ALLFIT software. *Bars*, range of values observed at each concentration.

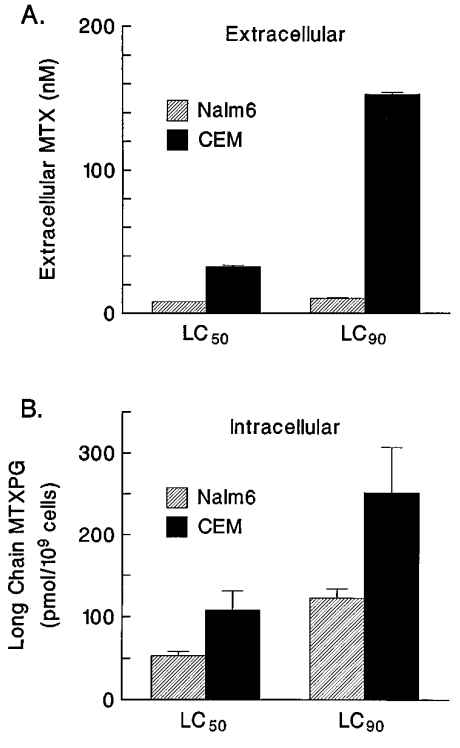

Fig. 10. Comparison of extracellular MTX concentration and intracellular long-chain MTXPG content producing 50% (LC_{50}) and 90% (LC_{90}) cell kill at 48 hr (24 hr after a continuous 24-hr exposure to MTX; see Fig. 5). A, Mean extracellular MTX concentration at the LC_{50} and LC_{90} for NALM6 (▨) and CEM (■). B, Mean intracellular long-chain MTXPG accumulation after 24-hr exposure to the extracellular MTX concentrations corresponding to the LC_{50} and LC_{90}. *Error bars*, upper range of observations for each mean value.

ml/min/m^2 (38). These data are consistent with the 5.0 g/m^2 dosages of MTX that are being empirically evaluated in children with T-lineage ALL (39) and with previous clinical data indicating that a MTX dosage of 1.0 g/m^2 may be too low for many children with B-lineage ALL (40).

It must be noted that the current *in vitro* studies were limited to only two human leukemia cell lines and that childhood ALL is a heterogenous disease with numerous lineage and genetic subtypes (32). Nevertheless, there was great similarity between the lineage differences observed *in vitro* and in patients. For example, $MTXPG_{4-6}$ accumulation was 4.3 times greater in NALM6 than CEM at 1.0 μM MTX and 2.7 times greater at 5.0 μM (Fig. 3), which is similar to the differences observed *in vivo* in lymphoblasts of patients with B-lineage versus T-lineage ALL (median $MTXPG_{4-6}$, 3.5 times higher in B-lineage after LDMTX and 3.1 times higher after HDMTX). Likewise, the maximum accumulation of $MTXPG_{4-6}$ was 3.6 times higher in patients with B-lineage ALL compared with T-lineage ALL (E_{max} in Fig. 1: 1568 versus 431 pmol/10^9 blasts). These data indicate that even with higher doses of MTX, intracellular accumulation of MTXPGs may remain lower in T-lineage compared with B-lineage lymphoblasts, related in part to the 3-fold lower constitutive expression of FPGS and the smaller increase in FPGS activity in T-lineage lymphoblasts after MTX exposure. These data also suggest saturation of mechanisms involved in MTXPG formation and accumulation in lymphoblasts in patients (Fig. 1) or *in vitro* (Fig. 4). However, there are relatively few patients with T-lineage ALL in this analysis (n = 18), and the data for patients with T-lineage ALL fits equally well with a linear model (Fig. 1). This observation raises questions about the rationale for very high doses of MTX (e.g., >5.0 g/m^2) that are used in some B-lineage ALL treatment protocols. The current study also suggests that $MTXPG_{4-6}$ accumulation approaches a steady state maximum more rapidly in B-lineage NALM6 than in T-lineage CEM lymphoblasts (Fig. 3), raising the possibility that optimal MTX infusion times may be different for B-lineage and T-lineage ALL. Because MTX infusion times of 2–48 hr are being used empirically to treat childhood ALL, this issue merits further clinical investigation. The current work has elucidated two potential mechanisms for lineage differences in MTXPG accumulation and cytotoxicity *in vivo*, providing insights into therapeutic strategies for circumventing these differences in patients with acute lymphoblastic leukemia.

Acknowledgments

We wish to thank L. McNinch, E. Melton, M. Chung, V. Parker, and M. Needham for their excellent technical assistance and the parents and patients who participated in this study.

References

1. Chabner, B. A., C. J. Allegra, G. A. Curt, N. J. Clendeninn, J. Baram, S. Koizumi, J. C. Drake, and J. Jolivet. Polyglutamation of methotrexate: is methotrexate a prodrug? *J. Clin. Invest.* **76:**907 (1985).
2. Shane, B. L. The role of folylpolyglutamate synthase in the regulation of folate and one-carbon metabolism. *Vitam. Horm.* **46:**263 (1989).
3. Jolivet, J., R. L. Schilsky, B. A. D. Bailey, J. C. Drake, and B. A. Chabner. Synthesis, retention, and biological activity of methotrexate polyglutamates in cultured human breast cancer cells. *J. Clin. Invest.* **70:**351 (1982).
4. Fry, D. W., J. C. Yalowich, and I. D. Goldman. Rapid formation of poly-γ-glutamyl derivatives of methotrexate and their association with dihydrofolate reductase as assessed by high-pressure liquid chromatography in Ehrlich ascites tumor cell in vitro. *J. Biol. Chem.* **259:**257 (1982).
5. Allegra, C. J., J. C. Drake, J. Jolivet, and B. A. Chabner. Inhibition of phosphoribosylamino-imidazolecarboxamide transformylase by methotrexate and dihydrofolic acid polyglutamates. *Proc. Natl. Acad. Sci. USA* **82:**4881 (1985).
6. McCloskey, D. E., J. J. McGuire, C. A. Russell, B. G. Rowan, J. R. Bertino, G. Pizzorno, and E. Mini. Decreased folylpolyglutamate synthetase activity as a mechanism of methotrexate resistance in CCRF-CEM human leukemia sublines. *J. Biol Chem.* **266:**6181 (1991).
7. Cowan, K. H., and J. Jolivet. A methotrexate-resistant human breast cancer cell line with multiple defects, including diminished formation of methotrexate polyglutamates. *J. Biol. Chem.* **259:**10793 (1984).
8. Pizzorno, G., Y.-M. Chang, J. J. McGuire, and J. R. Bertino. Inherent resistance of human squamous carcinoma cell lines to methotrexate as a result of decreased polyglutamylation of this drug. *Cancer Res.* **49:**5272 (1989).
9. Matherly, L. H., J. W. Taub, Y. Ravindranath, S. A. Proefke, S. C. Wong, P. Gimotty, and S. Buck. Elevated dihydrofolate reductase and impaired methotrexate transport as elements in methotrexate resistance in childhood acute lymphoblastic leukemia. *Blood* **85:**500 (1995).
10. Li, W.-W., J. T. Lin, W. P. Tong, T. M. Trippett, M. F. Brennan, and J. R. Bertino. Mechanisms of natural resistance to antifolates in human soft tissue sarcomas. *Cancer Res.* **52:**1434 (1992).
11. Fabre, I., G. Fabre, and I. D. Goldman. Polyglutamylation, an important element in methotrexate cytotoxicity and selectivity in tumor versus murine granulocytic progenitor cells *in vitro. Cancer Res.* **44:**3190 (1984).
12. Schuetz, J. D., E. H. Westin, L. H. Matherly, R. Pineus, P. S. Swerdlow, and I. D. Goldman. Membrane protein changes in an L1210 leukemia cell line with a translocation defect in the methotrexate-tetrahydrofolate cofactor transport courier. *J. Biol. Chem.* **264:**16261 (1989).
13. Srimatkandada, S., B. I. Schweitzer, B. A. Moroson, S. Dube, and J. R. Bertino. Amplification of a polymorphic dihydrofolate reductase gene expressing an enzyme with decreased binding to methotrexate in a human colon carcinoma cell line, HCT-8R4, resistant to this drug. *J. Biol. Chem.* **264:**3524 (1989).
14. Alt, F. W., R. E. Kellems, J. R. Bertino, and R. T. Schimke. Selective multiplication of dihydrofolate reductase genes in methotrexate-resistant variants of cultured murine cells. *J. Biol. Chem.* **253:**1357 (1978).
15. Wang, Y., J. A. Dias, Z. Nimec, R. Rotundo, B. M. O'Connor, J. Freisheim, and J. Galivan. The properties and function of *gamma*-glutamyl hydrolase and poly-*gamma*-glutamate. *Adv. Enzyme Regul.* **33:**207 (1993).
16. Goker, E., J. T. Lin, T. Trippett, Y. Elisseyeff, W. P. Tong, D. Niedzwiecki, C. Tan, P. Steinherz, B. I. Schweitzer, and J. R. Bertino. Decreased polyglutamylation of methotrexate in acute lymphoblastic leukemia blasts in adults compared to children with this disease. *Leukemia* **7:**1000 (1993).
17. Whitehead, V. M., M. J. Vuchich, S. J. Lauer, D. Mahoney, A. J. Carroll, J. J. Shuster, and D. J. Pullen. Accumulation of high levels of methotrexate polyglutamates in lymphoblasts from children with hyperdiploid (>50 chromosomes) B-lineage acute lymphoblastic leukemia: a Pediatric Oncology Group study. *Blood* **80:**1316 (1992).
18. Synold, T. W., M. V. Relling, J. M. Boyett, G. K. Rivera, J. T. Sandlund, H. Mahmoud, W. M. Crist, C.-H. Pui, and W. E. Evans. Blast cell methotrexate-polyglutamate accumulation in vivo differs by lineage, ploidy, and methotrexate dose in acute lymphoblastic leukemia. *J. Clin. Invest.* **94:** 1996 (1994).
19. Barredo, J. C., T. W. Synold, J. Laver, M. V. Relling, C.-H. Pui, D. G. Priest, and W. E. Evans. Differences in constitutive and post-methotrexate folylpolyglutamate synthetase activity in B-lineage and T-lineage leukemia. *Blood* **84:**564 (1994).
20. Masson, E., M. V. Relling, T. W. Synold, Q. Liu, J. D. Schuetz, J. T. Sandlund, C.-H. Pui, and W. E. Evans. Accumulation of methotrexate polyglutamates in lymphoblasts is a determinant of antileukemic effects in vivo: a rationale for high-dose methotrexate. *J. Clin Invest.* **97:**73 (1996).
21. Matherly, L. H., J. D. Schuetz, E. Westin, and I. D. Goldman. A method for the synchronization of cultured cells with aphidicolin: application to the large-scale synchronization of L1210 cells and the study of the cell cycle regulation of thymidylate synthase and dihydrofolate reductase. *Anal. Biochem.* **182:**338 (1989).
22. Garrow, T. A., A. Admon, and B. Shane. Expression cloning of a human cDNA encoding folylpoly(gamma-glutamate) synthetase and determination of its primary structure. *Proc. Natl. Acad. Sci. USA* **89:**9151 (1992).
23. Schuetz, J. D., S. Kauma, and P. S. Guzelian. Identification of the fetal liver cytochrome CYP3A7 in human endometrium and placenta. *J. Clin. Invest.* **42:**1018 (1993).
24. Antonsson, B., J. Barredo, and R. G. Moran. A microassay for mammalian folylpolyglutamate synthetase. *Anal. Biochem.* **186:**8 (1990).
25. Kamen, B. A., and N. Winick. Analysis of methotrexate polyglutamate derivatives in vivo. *Methods Enzymol.* **122:**339 (1986).
26. Hurwitz, R., J. Hozier, T. LeBien, J. Minowada, K. Gajl-Peczalska, I. Kubonishi, and J. Kersey. Characterization of a leukemia cell line of the Pre-B phenotype. *Int. J. Cancer* **23:**174 (1979).
27. Campana, D., A. Manabe, and W. E. Evans. Stroma-supported immunocytometric assay (SIA): a novel method for testing the sensitivity of acute lymphoblastic leukemia cells to cytotoxic drugs. *Leukemia* **7:**482 (1993).
28. DeLean, A., P. J. Munson, and D. Rodbord. Simultaneous analysis of families of sigmoid curves: application to bioassay, radioligand assay, and physiological dose-response curves. *Am. J. Physiol.* **235:**E97 (1978).
29. Chomcynski, P., and N. Sacchi. Single-step method of RNA isolation by acid guanidium thiocyanate-phenol-chloroform extraction. *Anal. Biochem.* **162:**156 (1987).
30. Schuetz, J. D., D. L. Beach, and P. S. Guzelian. Selective expression of cytochrome P450 CYP3A mRNAs in embryonic and adult human liver. *Pharmacogenetics* **4:**11 (1994).
31. Schuetz, J. D., K. M. Gorse, I. D. Goldman, and E. H. Westin. Transient inhibition of DNA synthesis by 5-fluorodeoxyuridine leads to overexpression of dihydrofolate reductase with increased frequency of methotrexate resistance. *J. Biol. Chem.* **263:**7708 (1988).
32. Pui, C.-H., F. G. Behm, and W. M. Crist. Clinical and biological relevance of immunologic marker studies in childhood acute lymphoblastic leukemia. *Blood* **82:**343 (1993).
33. Rivera, G. K., S. C. Raimondi, M. L. Hancock, F. G. Behm, C.-H. Pui, M. Abromowitch, J. Mirro, J. S. Ochs, A. T. Look, D. L. Williams, S. B. Murphy, G. V. Dahl, D. K. Kalwinsky, W. E. Evans, L. E. Kun, J. V. Simone, and W. M. Crist. Improved outcome in childhood acute lymphoblastic leukaemia with reinforced early treatment and rotational combination chemotherapy. *Lancet* **337:**61 (1991).
34. Moran, R. G., and P. D. Colman. Measurement of folylpolyglutamate synthetase in mammalian tissues. *Anal. Biochem.* **140:**326 (1984).
35. Barredo, J., and R. G. Moran. Determinants of antifolate cytotoxicity: folylpolyglutamate synthetase activity during cellular proliferation and development. *Mol. Pharmacol.* **42:**687 (1992).
36. Fort, D. W., R. H. Lark, A. K. Smith, M. Marling-Cason, S. D. Weitman, B. Shane, and B. A. Kamen. Accumulation of 5-methyltetrahydrofolic acid and folylpolyglutamate synthetase expression by mitogen stimulated human lymphocytes. *Br. J. Haematol.* **84:**595 (1993).
37. White, J. C., S. Loftfield, and I. D. Goldman. The mechanism of action of methotrexate. III. Requirement of free intracellular methotrexate for maximal expression of (^{14}C)-formate incorporation into nucleic acids and proteins. *Mol. Pharmacol.* **11:**287 (1975).
38. Relling, M. V., D. Fairclough, D. Ayers, W. R. Crom, J. H. Rodman, C.-H. Pui, and W. E. Evans. Patient characteristics associated with high-risk methotrexate concentrations and toxicity. *J. Clin. Oncol.* **12:**1667 (1994).
39. Reiter, A., M. Schrappe, W. D. Ludwig, W. Hiddemann, S. Sauter, G. Henze, M. Zimmerman, F. Lampert, W. Havers, D. Niethammer, E. Odenwald, J. Ritter, G. Mann, K. Welte, H. Gadner, and H. Riehm. Chemotherapy in 998 unselected childhood acute lymphoblastic leukemia patients: results and conclusions of the multicenter trial ALL-BFM 86. *Blood* **84:** 3122 (1994).
40. Evans, W. E., W. R. Crom, M. Abromowitch, R. Dodge, A. T. Look, W. P. Bowman, S. L. George, and C.-H. Pui. Clinical pharmacodynamics of high-dose methotrexate in acute lymphocytic leukemia. *N. Engl. J. Med.* **314:**471 (1986).

Send reprint requests to: Dr. William E. Evans, Pharmaceutical Sciences, St. Jude Children's Research Hospital, 332 N. Lauderdale Street, Memphis, TN 38101. E-mail: william.evans@stjude.org